The Double-Generalized Gamma Distribution and its Application to V2V Communications

Petros S. Bithas[1], Athanasios G. Kanatas[1], Daniel B. da Costa[2], Prabhat K. Upadhyay[3], and Ugo S. Dias[4]
[1]Department of Digital Systems, University of Piraeus, Greece
[2]Department of Computer Engineering, Federal University of Ceará (UFC), Sobral, CE, Brazil
[3]Discipline of Electrical Engineering, Indian Institute of Technology Indore, Madhya Pradesh, India
[4]Department of Electrical Engineering, University of Brasília, DF, Brazil
e-mail: {pbithas;kanatas}@unipi.gr, danielbcosta@ieee.org, pkupadhyay@iiti.ac.in, ugodias@ieee.org

***Abstract*—In this paper, important statistical properties of the double-generalized Gamma (dGG) distribution, a generic model that has been used for modeling the double-scattering radio propagation fading conditions, are obtained and investigated. In this context, useful statistical metrics, such as the probability density function, cumulative distribution function, and the moments, are derived. Moreover, the second-order statistics of this distribution are also analytically studied for the first time. Based on them, exact expressions for the outage probability, the average symbol error probability, and the capacity of a transmit antenna selection system operating in a vehicle-to-vehicle (V2V) communication environment are obtained. In addition, the level crossing rate and the average fade duration are studied. Simplified asymptotic closed-form expressions have been also obtained and used to investigate the diversity and coding gains.**

I. Introduction

With the rapid growth of the information and communication technologies (ICT), vehicles have been equipped with a plethora of sensors, onboard computers, and communication units, resulting to what is known as connected vehicles. The application of ICT to the road transport sector is expected to provide improvements regarding the environmental performance, efficiency, safety, and security [1]. In this context, different types of communications have appeared, including vehicle-to-vehicle (V2V) and vehicle-to-infrastructure (V2I). An important factor that plays a critical role on these systems' performance is the behavior of the wireless medium. In particular, in scenarios where both the source and the destination, of the transmitted signal, are moving, the so-called double-scattering fading model is observed [2]. Widely adopted distributions for modeling the double-bouncing scattering are the double-Rayleigh, -Nakagami, and -Weibull [3]–[6]. These distributions, provide good fit to experimental data for mobile-to-mobile communications, as it has been verified by many experimental campaigns, e.g., [7]. These are the reasons why many authors in the past have employed them for modeling this kind of environments, e.g., [8]–[10]. Nevertheless, all the aforementioned double-bouncing distributions represent special cases of the double-generalized Gamma (dGG), which by adjusting its three parameters can accurately model a plethora of different propagation conditions.

The dGG distribution is a generic and versatile fading channel model, which has recently been used for modeling the turbulence-induced fading in free-space optical communication systems, e.g., [11], [12]. In the context of wireless communications, many efforts have been devoted to analytically describe important statistical metrics of this distribution, which, in general, have led to approximated solutions, e.g., [13], [14]. However, important statistical characteristics of this generic distribution have not been studied yet, despite its effectiveness to describe a variety of V2V communication conditions. Such an analytical framework, can be used to study the performance of emerging and future wireless communication systems and this is the subject of the current paper. Furthermore, an attractive low complexity communication scheme that has recently employed in V2V communication studies is the transmit antenna selection (TAS), e.g., [15]–[17]. Based on this technique, the number of expensive radio frequency (RF) chains is considerably reduced, while an important performance improvement is achieved. However, to the best of the authors' knowledge, the performance of TAS in dGG fading channel has not been investigated in the past.

In this paper, important statistical characteristics for the dGG fading distribution are presented. Moreover, the second-order statistics of this generic distribution have also been studied for the first time. These novel expressions are applied to the performance analysis of TAS scheme operating in dGG fading environment. For this scenario, the performance has been studied in terms of outage probability (OP), symbol error probability (SEP), capacity, average output signal-to-noise ratio (SNR), level crossing rates (LCR), and average fade duration (AFD). This paper differs also from previous ones, since it employs the dGG fading distribution for the first time in V2V communication channels, exploiting thus its versatility to more accurately describe vehicular channel models.

The remainder of the paper is organized as follows. In Section II, the marginal and second-order statistics of the dGG distribution are presented. In Section III, the system and channel models of the TAS scheme are presented along with a stochastic analysis for the received SNR statistics. In Section IV, the derived statistics are employed for the performance evaluation, while in Section V, representative numerical examples are presented and discussed. In Section VI, some concluding remarks are provided.

II. Double-Generalized Gamma Statistics

A. Marginal Statistics

Let $R = G_1 \times G_2$ denote a random variable (RV) following the dGG distribution, in which G_i (with $i \in \{1,2\}$) are generalized-Gamma (GG) distributed RVs with probability density function (PDF) given by [18, eq. (1)]. Thus, the PDF of R can be written as

$$f_R(x) = \frac{2\beta \hat{\Omega}^{\frac{m_1+m_2}{2}}}{\Gamma(m_1)\Gamma(m_2)} x^{\frac{\beta}{2}(m_1+m_2)-1} K_{m_2-m_1}\left(2\sqrt{\hat{\Omega}} x^{\beta/2}\right), \quad (1)$$

in which β and m_1, m_2 are distribution's shaping parameters, $\hat{\Omega} = \frac{m_1 m_2}{\Omega_1 \Omega_2}$, $\Omega_i = \left(\mathbb{E}\left\langle G_i^2 \right\rangle \Gamma(m_i)/\Gamma(m_i + 2/\beta)\right)^{\beta/2} m_i$, $\mathbb{E}\langle\cdot\rangle$ denotes expectation, $\Gamma(\cdot)$ is the Gamma function [19, eq. (8.310/1)], and $K_v(\cdot)$ is the modified Bessel function of the second kind and order v [19, eq. (8.446)]. Based on its 3 shaping parameters, the dGG distribution can be efficiently utilized to provide excellent fit in different V2V channel measurements data, while its mathematical tractability can be exploited for analytical investigations. The cumulative distribution function (CDF) of R is given by

$$F_R(x) = \frac{\hat{\Omega}^{p_1}}{\Gamma(m_1)\Gamma(m_2)} x^{\beta p_1} \mathcal{G}_{1,3}^{2,1}\left(\hat{\Omega} x^{\beta} \Big|_{p_2, -p_2, -p_1}^{1-p_1}\right), \quad (2)$$

with $p_1 = \frac{m_1+m_2}{2}, p_2 = \frac{m_2-m_1}{2}$, and $\mathcal{G}_{p,q}^{m,n}[\cdot|\cdot]$ denoting the Meijer's G-function [19, eq. (9.301)]. It is noted that Meijer G-function is a built-in function in many mathematical software packages, e.g., Mathematica, Maple, and thus can be directly evaluated. Assuming integer values for m_2, (2) can be simplified to

$$F_R(x) = \frac{1}{\Gamma(m_2)}\Bigg(1 - \sum_{k_1=0}^{m_2-1} \frac{2\hat{\Omega}^{\frac{k_1+m_1}{2}}}{k_1!\Gamma(m_1)} x^{\frac{\beta}{2}(k_1+m_1)} \times K_{k_1-m_1}\left(2\hat{\Omega}^{1/2} x^{\beta/2}\right)\Bigg). \quad (3)$$

Furthermore, for $m_1 = n + 1/2$, with $n \in \mathbb{N}$, employing [19, eq. (8.468)], and performing some mathematical manipulations yield the following convenient expression for the CDF of R

$$F_R(x) = \frac{1}{\Gamma(m_2)}\Bigg[1 - \sum_{k_1,k_2=0}^{f(m_1,m_2)} D_1 \hat{\Omega}^{\frac{k_1+m_1-k_2-1/2}{2}} \times x^{\frac{\beta}{2}(k_1+m_1-k_2-1/2)} \exp\left(-2\sqrt{\hat{\Omega}} x^{\beta/2}\right)\Bigg], \quad (4)$$

in which $\sum_{k_1,k_2=0}^{f(m_1,m_2)} = \sum_{k_1=0}^{m_2-1} \sum_{k_2=0}^{|k_1-m_1|-1/2}$, $D_1 = \frac{\sqrt{\pi}/k_1!}{\Gamma(m_1) k_2! 2^{2k_2}} \frac{\left(|k_1-m_1|-\frac{1}{2}+k_2\right)!}{\left(|k_1-m_1|-\frac{1}{2}-k_2\right)!}$. Finally, the n_1th order moment of R is given by

$$\mu_R(n_1) = \frac{\hat{\Omega}^{-\frac{n_1}{\beta}}}{\Gamma(m_1)\Gamma(m_2)} \Gamma\left(m_1 + \frac{n_1}{\beta}\right) \Gamma\left(m_2 + \frac{n_1}{\beta}\right). \quad (5)$$

B. Second-Order Statistics

Let $R(t)$ be a dGG process with marginal PDF given by (1). Moreover, let $\dot{R}$ denote the time derivative of R, i.e., $\dot{R}(t) = dR(t)/dt$, at time t. Since the dGG random process is a product of two independent GG random processes, the joint PDF of $R(t)$ and $\dot{R}(t)$ can be expressed as [20]

$$f_{R\dot{R}}(x,\dot{x}) = \int_0^\infty \int_{-\infty}^\infty \frac{1}{y^2} f_{G_1\dot{G}_1}\left(\frac{x}{y}, \frac{\dot{x}}{y} - \frac{\dot{y}x}{y^2}\right) f_{G_2\dot{G}_2}(y,\dot{y})\, dy d\dot{y}, \quad (6)$$

in which $f_{G_i\dot{G}_i}(\cdot,\cdot)$ represents the joint PDF of the GG random process $G_i(t)$ and its derivative $\dot{G}_i(t)$, which has been derived in [18, eq. (24)]. Assuming $m_1 = m_2 = m, \Omega_1 = \Omega_2 = \Omega$, substituting [18, eq. (24)] in (6), using [19, eq. (3.323/2)], and performing some mathematical manipulations, the following expression for the joint PDF of $R(t)$ and $\dot{R}(t)$ is deduced

$$f_{R\dot{R}}(x,\dot{x}) = \frac{\beta^2 m^{2m+0.5} x^{\beta(m+0.5)-2}}{\sqrt{2\pi}\omega \Omega^{2m+0.5}\Gamma(m)^2} \times \int_0^\infty \frac{y^{-1}}{\sqrt{x^\beta y^{-1} + y}} \exp\left(-\frac{m}{\Omega} y\right) \exp\left[\frac{m\beta^2 \dot{x}^2 x^{2\beta-2}}{(x^\beta + y^2)\, 2\omega^2 \Omega y}\right] \times \exp\left[-\frac{m x^\beta}{\Omega}\left(\frac{\beta^2 \dot{x}^2}{2\omega^2 x^2} + 1\right) y^{-1}\right] dy, \quad (7)$$

with ω denoting the frequency in radians per second. The integral in (7) can be easily evaluated using well-known mathematical software packages such as Mathematica or Matlab.

1) Level Crossing Rates: LCR is defined as the number of times per unit duration that a random process crosses a predefined threshold R_{th} in the negative direction, and mathematically is given as

$$N_R(R_{\text{th}}) = \int_0^\infty \dot{x} f_{R\dot{R}}(R_{\text{th}}, \dot{x})\, d\dot{x}. \quad (8)$$

Substituting (7) in (8) and using [19, eq. (3.310)] yield

$$N_R(R_{\text{th}}) = \frac{m^{2m-0.5}\omega}{\sqrt{2\pi}\Omega^{2m-0.5}\Gamma(m)^2} R_{\text{th}}^{\beta(m-0.5)} \int_0^\infty \frac{y^{-3/2}}{\sqrt{R_{\text{th}}^\beta + y^2}} \times \exp\left(-\frac{m}{\Omega} y\right) \exp\left(-\frac{m R_{\text{th}}^\beta}{\Omega} y^{-1}\right) \left(y^2 + R_{\text{th}}^\beta\right) dy. \quad (9)$$

Assuming $\beta = 2$, (9) simplifies to the LCR of the double-Nakagami distribution [8, eq. (9)].

2) Average Time Below Level: The average time below level (ATBL) is defined as the average length of the intervals for which $R(t)$ is below the threshold R_{th} divided by the LCR, which mathematical is expressed as

$$\alpha(R_{\text{th}}) = \frac{F_R(R_{\text{th}})}{N_R(R_{\text{th}})}, \quad (10)$$

in which $F_R(R_{\text{th}})$ and $N_R(R_{\text{th}})$ are given by (3) and (9), respectively. It should be noted that most of the previous derived expressions have never been reported in the open technical literature.

III. TAS Statistics

A. System Model

Considering a low complexity communication system with L transmit antennas and one receive antenna, operating in a V2V communication environment that is modeled by the dGG fading distribution. The receiver selects the transmit antenna providing the highest received SNR value, via an error-free and zero-delay feedback link. Assuming identical parameters for all diversity links, the instantaneous output SNR can be expressed as

$$\gamma_{\text{out}} = \max\{\gamma_1, \gamma_2, \ldots, \gamma_L\}, \tag{11}$$

in which $\gamma_\ell = R_\ell^2 \frac{E_s}{N_0}$ is associated with the ℓth transmitting antenna ($\ell \in \{1, 2, \ldots, L\}$), E_s is the transmitted symbol energy, N_0 is the noise variance, and R_ℓ is a dGG RV with marginal PDF given by (1). The corresponding PDF and CDF of γ_ℓ are, respectively, given by

$$\begin{aligned} f_{\gamma_\ell}(\gamma) =& \frac{\beta \hat{\gamma}^{\frac{m_1+m_2}{2}}}{\Gamma(m_1)\Gamma(m_2)} \\ &\times \gamma^{\frac{\beta}{4}(m_1+m_2)-1} K_{m_2-m_1}\left(2\sqrt{\hat{\gamma}}\gamma^{\beta/4}\right), \end{aligned} \tag{12}$$

$$\begin{aligned} F_{\gamma_\ell}(\gamma) =& \frac{1}{\Gamma(m_2)}\left[1 - \sum_{k_1,k_2=0}^{f(m_1,m_2)} D_1 \hat{\gamma}^{\frac{k_1+m_1-k_2-1/2}{2}} \right. \\ &\left. \times \gamma^{\frac{\beta}{4}(k_1+m_1-k_2-1/2)} \exp\left(-2\sqrt{\hat{\gamma}}\gamma^{\beta/4}\right)\right], \end{aligned} \tag{13}$$

with $\hat{\gamma} = \left[\frac{\Gamma(m_1)\Gamma(m_2)\overline{\gamma}_{b_1}\overline{\gamma}_{b_2}}{\Gamma(m_1+2/\beta)\Gamma(m_2+2/\beta)}\right]^{-\frac{\beta}{2}}$ and $\overline{\gamma} = \mathbb{E}\left\langle R_\ell^2\right\rangle \frac{E_s}{N_0} = \overline{\gamma}_{b_1}\overline{\gamma}_{b_2}$. As far as channel modeling is concerned, capitalizing on the generic form of the dGG distribution, the accurate modeling of several double-bouncing fading conditions is allowed. More specifically, in (12), m_i and β are related with the severity of the fading, i.e., higher values for m_i, β denote lighter fading conditions. For the system under consideration, the CDF of γ_{out} is

$$F_{\gamma_{\text{out}}}(\gamma) = \left[F_{\gamma_\ell}(\gamma)\right]^L. \tag{14}$$

Using (13) in (14), employing first the binomial identity, then multinomial identity, and after some mathematical procedure, the following convenient closed-form expression for $F_{\gamma_{\text{out}}}(\gamma)$ is attained

$$\begin{aligned} F_{\gamma_{\text{out}}}(\gamma) = & \sum_{q,t_i,v_{i,j}}^{L} \frac{1}{\Gamma(m_2)^L}\binom{L}{q} D_2 \hat{\gamma}^{d_2} \\ & \times \gamma^{\frac{\beta d_2}{2}} \exp\left(-2q\hat{\gamma}^{1/2}\gamma^{\beta/4}\right), \end{aligned} \tag{15}$$

in which

$$\sum_{q,t_i,v_{i,j}}^{L} = \sum_{q=0}^{L} \sum_{\substack{t_1,\cdots,t_{m_2}=0 \\ t_1+\ldots+t_{m_2}=q}}^{q} \cdots \sum_{\substack{v_{1,1},\cdots,v_{m_2,|m_2-1-m_1|+\frac{1}{2}}=0 \\ v_{1,1}+\cdots+v_{m_2,|m_2-1-m_1|+\frac{1}{2}}=t_{m_2}}}^{t_{m_2}},$$

$$\begin{aligned} D_2 =& \frac{(-1)^q q!}{t_1!\cdots t_{m_2}!}\left[\frac{\sqrt{\pi}}{\Gamma(m_1)}\right]^q \\ &\times \frac{t_1!\cdots t_{m_2}!}{v_{1,1}!\cdots v_{1,m_1+\frac{1}{2}}!\cdots v_{m_2,1}!\cdots v_{m_2,|m_2-1-m_2|+\frac{1}{2}}!} \\ &\times \prod_{k=0}^{m_2-1}\prod_{p=0}^{|k-m_1|-\frac{1}{2}}\left[\frac{(|k-m_1|-\frac{1}{2}+p)!}{k!p!(|k-m_1|-\frac{1}{2}-p)!2^{2p}}\right]^{v_{k+1,p+1}}, \end{aligned}$$

$$d_2 = \sum_{k=0}^{m_2-1}\sum_{p=0}^{|k-m_1|-\frac{1}{2}}\left(\frac{k+m_1-p-1/2}{2}\right)v_{k+1,p+1}.$$

The corresponding PDF expression is given by $f_{\gamma_{\text{out}}}(\gamma) = L f_{\gamma_\ell}(\gamma) F_{\gamma_\ell}(\gamma)^{L-1}$. Substituting (15) in this expression and doing some mathematical manipulations yield the following expression for the PDF of γ_{out}

$$\begin{aligned} f_{\gamma_{\text{out}}}(\gamma) = & L f_{\gamma_i}(\gamma) \sum_{q,t_i,v_{i,j}}^{L-1} \frac{1}{\Gamma(m_2)^{L-1}}\binom{L-1}{q} \\ & \times D_2 \hat{\gamma}^{d_2} \gamma^{\frac{\beta d_2}{2}} \exp\left(-2q\hat{\gamma}^{1/2}\gamma^{\beta/4}\right). \end{aligned} \tag{16}$$

B. Asymptotic Analysis

The exact expression for $F_{\gamma_{\text{out}}}(\gamma)$ does not provide a direct physical insight of the system's performance. In order to provide a simplified expression, the main concern is to derive an asymptotic *closed-form* expression for $F_{\gamma_{\text{out}}}(\gamma)$. Therefore, assuming higher values of $\overline{\gamma}$, using $\gamma(a, z_1) \simeq z_1^a$ [21, eq. (06.07.06.0004.01)], a closed-form asymptotic expression for the CDF of γ_{out} can be obtained as

$$F_{\gamma_{\text{out}}}(\gamma) \simeq \left(\frac{\Gamma(m_1-m_2)\gamma^{\frac{\beta}{2}m_2}\hat{\gamma}^{m_2}}{\Gamma(m_1)\Gamma(m_2)m_2}\right)^L. \tag{17}$$

In the next section, easy-to-compute closed-form expressions for various performance indicators are obtained. It is worth remarking that these expressions can only be derived using the mathematical framework provided above.

IV. Performance Analysis

In this section, using the previously derived results, analytical expressions for important performance metrics of the quality of service (QoS) are derived, such as the OP, the SEP, the average capacity, the average output SNR, the LCR, and the AFD.

A. Outage Probability

OP is defined as the probability that the output SNR falls below a predetermined threshold γ_{T} and is given by $P_{\text{out}} = F_{\gamma_{\text{out}}}(\gamma_{\text{T}})$, with $F_{\gamma_{\text{out}}}(\gamma_{\text{T}})$ given by (15).

Diversity and Coding Gains: At the high SNR regime, the OP can be characterised by two parameters: diversity gain, G_d, and coding gain, G_c, i.e., $P_{\text{out}}^{\infty} \simeq \left(G_c\overline{\gamma}_{b_i}\right)^{-G_d}$. Thus, based on (17), it can be concluded that $G_C = \left[\frac{\Gamma(m_1-m_2)[\Gamma(m_1+2/\beta)\Gamma(m_2+2/\beta)]^{m_2\frac{\beta}{2}}\gamma_T^{\frac{\beta}{2}m_2}}{[\Gamma(m_1)\Gamma(m_2)]^{m_2\frac{\beta}{2}+1}m_2}\right]^{-\frac{1}{m_2\beta}}$ and $G_d = m_2\beta L$. Therefore, the diversity gain depends on the fading severity, modeled by the shaping parameters m_2, β, as well as the number of transmit antennas L.

B. Symbol Error Probability

The SEP is one of the most important performance measures, the minimization of which is the main objective in designing wireless communication systems. For evaluating the SEP, the CDF-based approach is employed as follows [22]

$$\bar{P}_e = \int_0^\infty (-P_e^{'}) F_{\gamma_{\text{out}}}(\gamma) d\gamma, \tag{18}$$

in which $(-P_e^{'})$ denotes the negative derivative of the conditional error probability. In particular, for binary phase shift keying (BPSK) or binary frequency shift keying (BFSK) $P_e = \alpha Q(\sqrt{b\gamma})$, with $Q(\cdot)$ being the area under the tail of the Gaussian PDF [22, eq. (2-1-97)], while for differentially BPSK (DBPSK) $P_e = \alpha \exp(-b\gamma)$. For the BPSK case, the following closed-form expression for SEP has been obtained

$$\bar{P}_e = \sum_{q,t_i,v_{i,j}}^{L} \frac{1}{\Gamma(m_2)^L} \binom{L}{q} D_2 \hat{\gamma}^{d_2} \frac{\alpha\sqrt{b}}{\sqrt{8\pi}} D_3\left(\frac{b}{2}, \frac{1}{2}\right), \tag{19}$$

with

$$D_3(x,y) = \frac{(4\kappa)^{1/2}\lambda^{\frac{\beta}{2}d_2 - y + \frac{1}{2}}}{x^{\frac{\beta}{2}d_2 + y}(2\pi)^{\frac{1}{2}(\lambda+4\kappa-2)}} \times \mathcal{G}^{4\kappa,\lambda}_{\lambda,4\kappa}\left(\left(\frac{q\hat{\gamma}}{2\kappa}\right)^{4\kappa}\left(\frac{\lambda}{x}\right)^{\lambda} \middle| \begin{matrix}\Delta\left(\lambda, 1-\frac{\beta}{2}d_2 - y\right) \\ \Delta(4\kappa, 0)\end{matrix}\right),$$

and $\Delta(x,y) = \frac{y}{x}, \frac{y+1}{x}, \cdots, \frac{y+x-1}{x}$. In $D_3(x,y)$, parameters λ, κ represent two minimum positive integers such that $\beta = \lambda/\kappa$. Due to space constraints, the proof has been omitted here. It is noted that (19) generalizes previous known result [10, eq. (20)]. For the DBPSK scheme, by following a similar approach as the one used for deriving the SEP of BPSK, the following expression is deduced

$$\bar{P}_e = \sum_{q,t_i,v_{i,j}}^{L} \frac{1}{\Gamma(m_2)^L} \binom{L}{q} D_2 \hat{\gamma}^{d_2} ab D_3(b, 1). \tag{20}$$

Asymptotic Analysis: Using (17) in (18), the asymptotic expression for the SEP of DBPSK can be directly evaluated as $\overline{P}_e \simeq \left(\frac{\Gamma(m_1 - m_2)\hat{\gamma}^{m_2}}{b^{\beta m_2/2}\Gamma(m_1)\Gamma(m_2)}\right)^L a\Gamma\left(1 + \frac{\beta m_2 L}{2}\right)$.

C. Average Channel Capacity

Channel capacity is defined as

$$\hat{C} = \frac{BW}{\ln(2)} \int_0^\infty \frac{1 - F_{\gamma_{\text{out}}}(\gamma)}{1+\gamma} d\gamma, \tag{21}$$

in which BW denotes the signal's transmission bandwidth. The following closed-form expression can be derived for the capacity

$$\hat{C} = \sum_{q,t_i,v_{i,j}}^{L} \frac{(-1)^{-1} BW}{\ln(2)\Gamma(m_2)^L} \binom{L}{q} D_2 \hat{\gamma}^{d_2} D_4, \tag{22}$$

with q starting at 1 and

$$D_4 = \frac{(4\kappa)^{1/2}}{(2\pi)^{\lambda + 2\kappa - \frac{3}{2}}} \mathcal{G}^{4\kappa+\lambda,\lambda}_{\lambda,4\kappa+\lambda}\left(\left(\frac{q\hat{\gamma}}{2\kappa}\right)^{4\kappa} \middle| \begin{matrix}\Delta\left(\lambda, -\frac{\beta}{2}d_2\right) \\ \Delta(4\kappa,0), \Delta\left(\lambda, -\frac{\beta}{2}d_2\right)\end{matrix}\right). \tag{23}$$

Due to space constraints, the proof has been omitted here.

D. Average Output SNR

The average output SNR is a performance metric providing excellent indication of the overall system's fidelity. For the scheme under consideration, it is defined as

$$\mathbb{E}\langle\gamma_{\text{out}}\rangle = \int_0^\infty \left[1 - F_{\gamma_{\text{out}}}(\gamma)\right] d\gamma. \tag{24}$$

Substituting (15) in (24), and using [19, eq. (3.351/3)], we arrive at the following expression

$$\mathbb{E}\langle\gamma_{\text{out}}\rangle = \sum_{q,t_i,v_{i,j}}^{L} \frac{(-1)^{-1}}{\Gamma(m_2)^L} \binom{L}{q} D_2 \frac{2^{2-\frac{4}{\beta}-2d_2}\Gamma\left(\frac{4}{\beta} + 2d_2\right)}{\beta\hat{\gamma}^{\frac{2}{\beta}} q^{\frac{2(2+\beta d_2)}{\beta}}}. \tag{25}$$

E. Level Crossing Rate and Average Fade Duration

1) Level Crossing Rate: Assuming i.i.d. fading conditions, and using (9) as well as (2), the LCR can be evaluated as

$$N_T(R_{\text{th}}) = L N_R(R_{\text{th}}) F_R(R_{\text{th}})^{L-1}. \tag{26}$$

For $\beta = 2$, (26) simplifies to previous known result [9, eq. (14)]. It is noted that since $R(t)$ denotes a fading process, ω denotes the maximum Doppler shift in radians per second, which depends on the speed of vehicle and the carrier frequency. For example, in a real world example, assuming ITS-G5 standard and a vehicle speed equal to 80 km/h, $\omega = 2745.75$ rad/s. Moreover, a simpler expression for N_R can be extracted for higher values of Ω. In particular, based on (7), using [19, eq. (3.351/3)] as well as [23, eq. (2.3.7/8)], the following closed-form approximated expression for the LCR is obtained

$$\begin{aligned} N_R(R_{\text{th}}) \approx &\left(\frac{m^m/\sqrt{\pi}}{\Omega^m\Gamma(m)}\right)^2 \sqrt{\Omega/(2m)}\,\omega R_{\text{th}}^{\beta(m-1/4)} \\ &\times \left[\frac{2\pi\Omega^{1/2}{}_1F_2\left(\frac{1}{2}; \frac{1}{4}, \frac{3}{4}; -\frac{m^2 R_{\text{th}}^{\beta}}{4\Omega^2}\right)}{\sqrt{m R_{\text{th}}^{\beta/2}}}\right. \\ &- 4\Gamma\left(\frac{3}{4}\right)^2 {}_1F_2\left(\frac{3}{4}; \frac{1}{2}, \frac{5}{4}; -\frac{m^2 R_{\text{th}}^{\beta}}{4\Omega^2}\right) \\ &\left.- \frac{m R_{\text{th}}^{\beta/2}\Gamma\left(-\frac{3}{4}\right)\Gamma\left(\frac{5}{4}\right){}_1F_2\left(\frac{5}{4}; \frac{3}{2}, \frac{7}{4}; -\frac{m^2 R_{\text{th}}^{\beta}}{4\Omega^2}\right)}{\Omega}\right], \end{aligned} \tag{27}$$

with ${}_1F_2(\cdot;\cdot,\cdot;\cdot)$ denoting the generalized hypergeometric function [21, eq. (07.22.02.0001.01)].

2) Average Fade Duration: The AFD is defined as the average length of time the fading envelope remains under R_{th}, once it crosses this value in the negative direction. Based on (10) and using (26), AFD can be expressed as

$$a_T(R_{\text{th}}) = \frac{F_R(R_{\text{th}})^L}{L N_R(R_{\text{th}}) F_R(R_{\text{th}})^{L-1}} = \frac{F_R(R_{\text{th}})}{L N_R(R_{\text{th}})}. \tag{28}$$

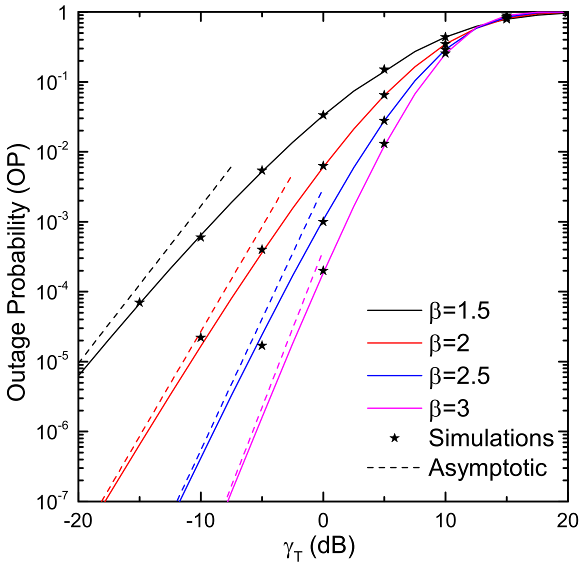

Fig. 1. OP vs γ_T for different values of β.

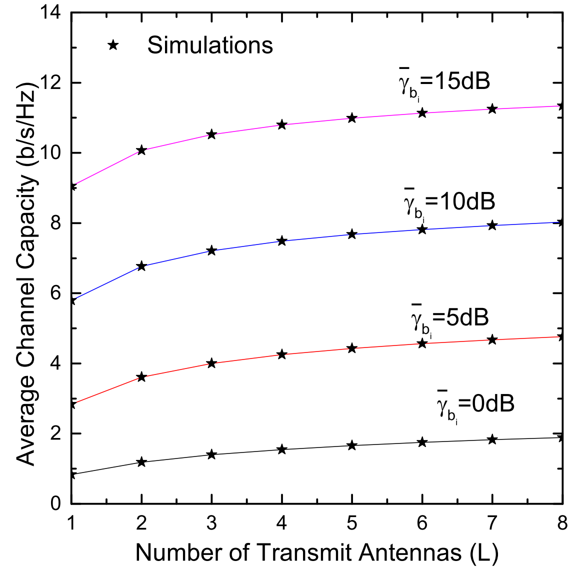

Fig. 3. Normalized channel capacity vs L for different values of $\overline{\gamma}_{b_i}$.

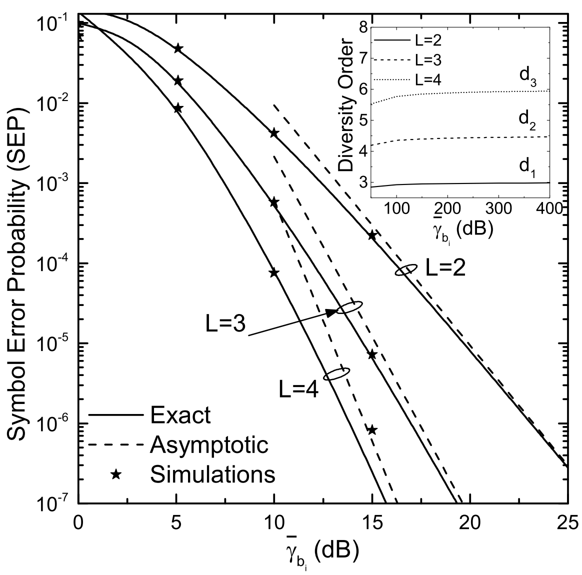

Fig. 2. SEP of DBPSK vs $\overline{\gamma}_{b_i}$ for different values of L.

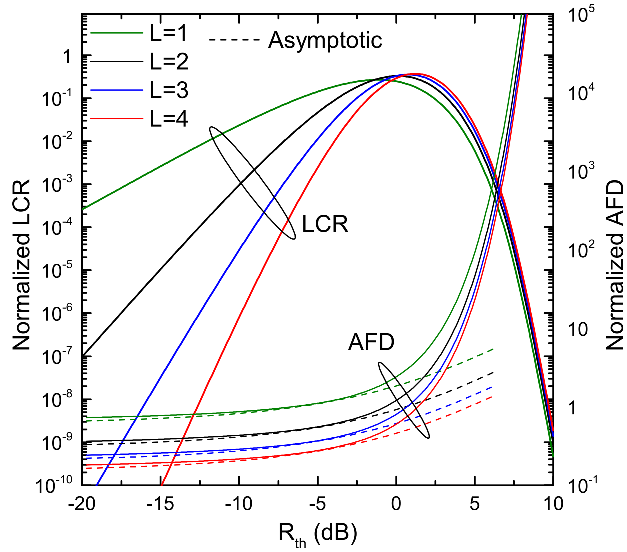

Fig. 4. Normalized LCR and AFD vs R_{th} for different values of L.

V. Numerical Results

In this section, several numerically evaluated performance results are presented and discussed. These results include performance comparisons of several TAS structures, employing various modulation formats and different V2V channel conditions. In Fig. 1, the OP is plotted as a function of γ_T for different values of the shaping parameter β. The following parameters were set: $m_1 = 1.5, m_2 = 1$, $L = 3$, $\overline{\gamma}_{b_i} = 5$dB. It is shown that the performance improves with the increase of β and/or a decrease of γ_T. In the same figure, it is shown that the asymptotic performance of the OP, which is also plotted, approximates quite well the exact one, especially for lower values of γ_T. In Fig. 2, considering DBPSK, the SEP is plotted as a function of $\overline{\gamma}_{b_i}$, for different values of L. The following parameters were set: $m_1 = 1.5, m_2 = 1$, $\beta = 1.5$, with $\lambda = 3, \kappa = 2$. It is shown that the SEP decreases with the increase of $\overline{\gamma}_{b_i}$ and L. It is noted that as L increases, the performance improves, with a decreased rate. In the same figure, the asymptotic SEP is also included, which approximates, at high SNR, quite well the exact performance. Finally, in the same figure, the diversity order, defined as $d = -\log\left(\overline{P}_{\mathrm{e}}\right)/\log\left(\mathrm{SNR}\right)$, is plotted as a function of $\overline{\gamma}_{b_i}$ for different values of the number of L. As depicted in this figure, as the SNR tends to infinity, the diversity order approaches $d_i = m_2\beta \cdot L$ (with $L \equiv \{2, 3, 4\}$ and $i = L - 1$), verifying the theoretical analysis presented in Section IV.

In Fig. 3, the normalized channel capacity is plotted as a function of the number of the transmitting antenna L, for different values of $\overline{\gamma}_{b_i}$. The following parameters were set:

$m_1 = 1.5, m_2 = 1, \beta = 2.5$, with $\lambda = 5$ and $\kappa = 2$. It is shown that the performance improves as the number antennas increases, with, however, a decreased rate. Moreover, it is also shown that the performance improvement is greater for lower values of $\overline{\gamma}_{b_i}$. It is noted that simulation performance results are also included in Figs. 1-3, verifying the validity of the proposed theoretical approach.

In Fig. 4, the normalized LCR, N_R/ω, is plotted as a function of normalized received envelope $R_{\rm th}/\Omega$ for different number of transmit antennas. The following parameters were used: $m_1 = 1.5, m_2 = 1$, $\beta = 2.1$, $\Omega = 0$ dB. As it is shown, for lower values of $R_{\rm th}$, the LCR decreases as L increases, with decreased rate. However, for higher values of $R_{\rm th}$, i.e., $R_{\rm th} > 0$ dB, the lower rate is obtained when $L = 1$. In the same figure, the normalized AFD is plotted as a function of $R_{\rm th}$. It is shown that for lower values of $R_{\rm th}$, the TAS system spends less time into deep fades. In other words, TAS crosses low values of $R_{\rm th}$ less often than single transmitting systems. Moreover, note that the asymptotic LCR approximates quite close the exact one, especially for lower values of $R_{\rm th}$.

VI. Conclusions

The performance of a TAS scheme operating in a V2V communication environment has been analytically investigated. For the purposes of the analysis, convenient expressions for important statistical metrics of the dGG distribution have been presented for the first time, including the PDF, CDF, and the moments. This distribution generalizes previous known ones that have been proposed for modeling the double-bouncing mechanism frequently occurring in mobile-to-mobile communications. In this context, the second-order statistics of the dGG model were also studied. Based on the derived expressions, the performance of the scheme under consideration has been investigated, using well-known metrics for the QoS, namely OP, SEP, capacity, the LCR, and the AFD. Moreover, asymptotic expressions have been also provided and used to study the diversity and coding gains. Finally, numerical results have been presented in order to investigate the performance of the system under consideration. In the journal version of this paper the impact of outdated channel state information on the system's QoS will be also studied.

Acknowledgement

This research has received funding from the European Union's Horizon 2020 research and innovation programme under "ROADART" Grant Agreement No 636565. The research work of P. K. Upadhyay was supported in part by the Young Faculty Research Fellowship of MeitY, Govt. of India. The work of U. S. Dias was partially supported by the Brazilian Ministry of Justice and Public Safety under grant TED-FUB-SENACON/MJ 001/2015.

References

[1] P. M. d'Orey and M. Ferreira, "ITS for sustainable mobility: A survey on applications and impact assessment tools," *IEEE Trans. Intell. Transp. Syst.*, vol. 15, no. 2, pp. 477–493, Apr. 2014.

[2] J. B. Andersen, "Statistical distributions in mobile communications using multiple scattering," in *Proc. 27th URSI General Assembly*, 2002.

[3] J. Salo, H. M. El-Sallabi, and P. Vainikainen, "Impact of double-Rayleigh fading on system performance," in *Proc. 1st IEEE ISWPC*, 2006.

[4] P. S. Bithas, K. Maliatsos, and A. G. Kanatas, "The bivariate double Rayleigh distribution for multichannel time-varying systems," *IEEE Wireless Commun. Lett.*, vol. 5, no. 5, pp. 524–527, Oct 2016.

[5] G. K. Karagiannidis, N. C. Sagias, and P. T. Mathiopoulos, "N*Nakagami: A novel stochastic model for cascaded fading channels," *IEEE Trans. Commun.*, vol. 55, no. 8, pp. 1453–1458, Aug. 2007.

[6] N. C. Sagias and G. S. Tombras, "On the cascaded Weibull fading channel model," *Journal of the Franklin Institute*, vol. 344, no. 1, 2007.

[7] E. Vinogradov, W. Joseph, and C. Oestges, "Measurement-based modeling of time-variant fading statistics in indoor peer-to-peer scenarios," *IEEE Trans. Antennas Propag.*, vol. 63, no. 5, pp. 2252–2263, May 2015.

[8] N. Zlatanov, Z. Hadzi-Velkov, and G. K. Karagiannidis, "Level crossing rate and average fade duration of the double Nakagami-m random process and application in MIMO keyhole fading channels," *IEEE Commun. Lett.*, vol. 12, no. 11, pp. 822–824, Nov. 2008.

[9] R. Khedhiri, N. Hajri, N. Youssef, and M. Patzold, "On the first- and second-order statistics of selective combining over double Nakagami-m fading channels," in *Proc. IEEE 80th VTC*, Sep. 2014.

[10] M. L. Ammari and S. Roy, "Performance analysis of diversity combining techniques in double-Rayleigh channels," in *Proc. ICNC*, Feb. 2016.

[11] H. AlQuwaiee, I. S. Ansari, and M. S. Alouini, "On the performance of free-space optical communication systems over double generalized gamma channel," *IEEE J. Sel. Areas Commun.*, vol. 33, no. 9, pp. 1829–1840, Sep. 2015.

[12] ——, "On the maximum and minimum of double generalized gamma variates with applications to the performance of free-space optical communication systems," *IEEE Trans. Veh. Technol.*, vol. 65, no. 11, pp. 8822–8831, Nov 2016.

[13] Y. Chen, G. K. Karagiannidis, H. Lu, and N. Cao, "Novel approximations to the statistics of products of independent random variables and their applications in wireless communications," *IEEE Trans. Veh. Technol.*, vol. 61, no. 2, pp. 443–454, Feb 2012.

[14] E. F. Abd-Elfattah, "Saddlepoint density and distribution functions for the ratio of two linear functions and the product of generalized gamma variates," *Communications in Statistics - Theory and Methods*, 2017.

[15] Z. Chen, J. Yuan, and B. Vucetic, "Analysis of transmit antenna selection/maximal-ratio combining in Rayleigh fading channels," *IEEE Trans. Veh. Technol.*, vol. 54, no. 4, pp. 1312–1321, Jul. 2005.

[16] S. O. Ata and I. Altunbas, "Joint relay and antenna selection in MIMO PLNC inter-vehicular communication systems over cascaded fading channels," *Wireless Personal Communications*, vol. 92, no. 3, pp. 901–923, 2017.

[17] P. S. Bithas, A. G. Kanatas, D. B. da Costa, and P. K. Upadhyay, "Transmit antenna selection in vehicle-to-vehicle time-varying fading channels," in *IEEE ICC*, May 2017.

[18] M. D. Yacoub, "The α-μ distribution: A physical fading model for the Stacy distribution," *IEEE Trans. Veh. Technol.*, vol. 56, no. 1, pp. 27–34, Jan. 2007.

[19] I. S. Gradshteyn and I. M. Ryzhik, *Table of Integrals, Series, and Products*, 6th ed. New York: Academic Press, 2000.

[20] A. Krantzik and D. Wolf, "Distribution of the fading intervals of modified Suzuki process," in *Proc. EUSIPCO*, Jan. 1990, pp. 361–364.

[21] The Wolfram Functions Site, 2017. [Online]. Available: http://functions.wolfram.com

[22] Y. Chen and C. Tellambura, "Distribution functions of selection combiner output in equally correlated Rayleigh, rician, and Nakagami-m fading channels," *IEEE Trans. Commun.*, vol. 52, no. 11, pp. 1948–1956, Nov. 2004.

[23] A. Prudnikov, Y. Brychkov, and O. Marichev, *Integrals and Series, Volume 1*. Gordon and Breach Science Publishers, 1986.